

## Supplementary Information

### Table of Contents

**Fig. S1** UV-Vis spectra of *R/S*-0.8-quasi films and *R/S*-0.4-quasi films.

**Fig. S2** X-ray photoelectron spectroscopy spectra (XPS) of a *R*-0.4-quasi film.

**Fig. S3** Enhanced GIWAXS pattern of *R*-0.4-quasi film.

**Fig. S4** SEM images of quasi-2D films.

**Fig. S5** AFM image area of quasi-2D films (2\*2  $\mu\text{m}^2$ ).

**Fig. S6** Raw and averaged *I-V* curves of *R/S*-0.2-quasi films.

**Fig. S7** Raw and averaged *I-V* curves of *R/S*-2D films.

**Fig. S8** Raw and averaged *I-V* curves of *R/S*-0.4-quasi films.

**Fig. S9** Electroluminescence performance of spin-LEDs.

**Fig. S10** Electroluminescence properties of the *rac*-LED.

**Table S1** Elemental analysis of quasi-2D film.

**Table S2** Summary of CP-EL Emitting LEDs Based on CISS.

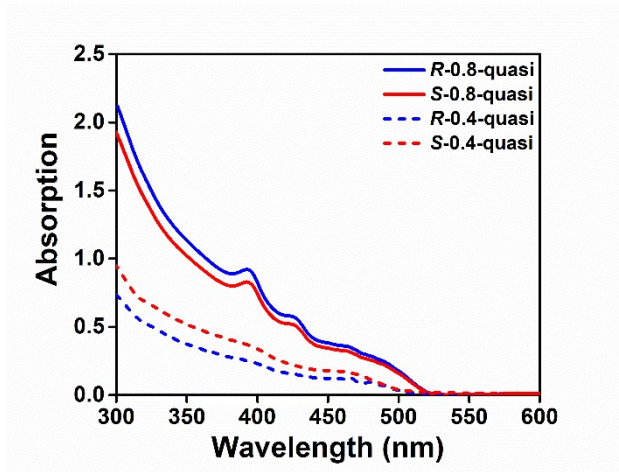


**Fig. S1.** UV-Vis spectra of *R/S*-0.8-quasi films and *R/S*-0.4-quasi films.

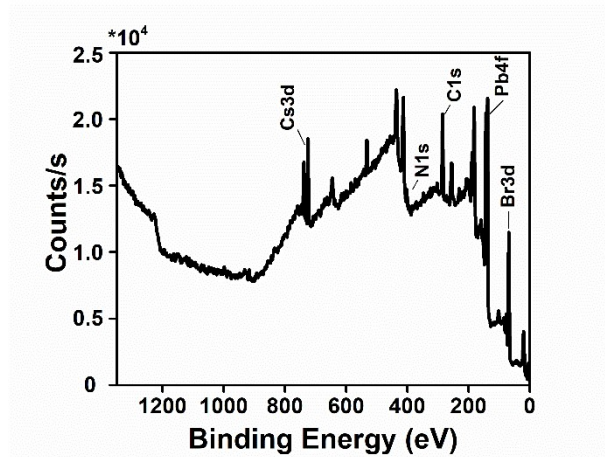


**Fig. S2** X-ray photoelectron spectroscopy spectra (XPS) of a R-0.4-quasi film.

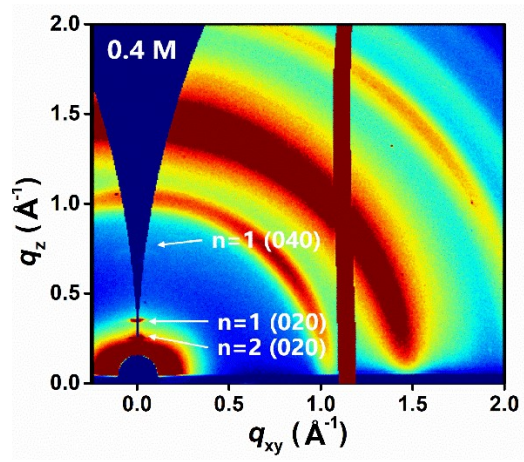


**Fig. S3** Enhanced GIWAXS pattern of R-0.4-quasi film.

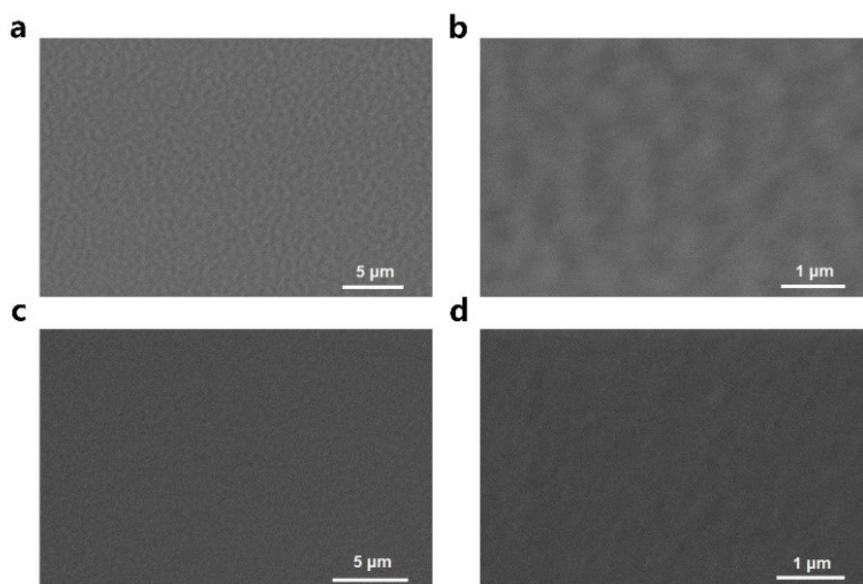


**Fig. S4** SEM images of quasi-2D films: **a, b** *R*-0.8-quasi film. **c, d** *R*-0.4-quasi film.

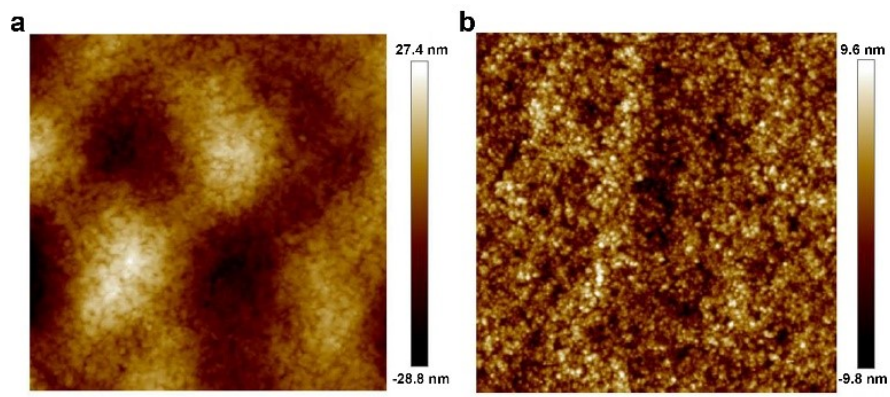


**Fig. S5** AFM image area of quasi-2D films ( $2 \times 2 \mu\text{m}^2$ ): **a** *R*-0.8-quasi film. **b** *R*-0.4-quasi film.

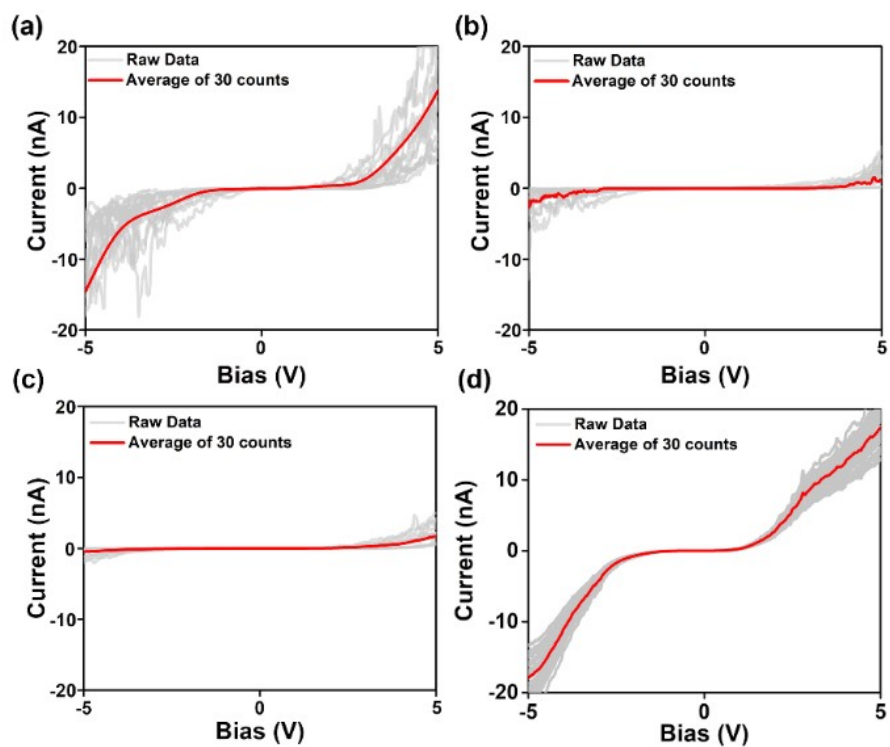


**Fig. S6** Raw and averaged  $I$ - $V$  curves obtained using the mCP-AFM for R-0.2-quasi film **a** Tip<sub>down</sub>, **b** Tip<sub>up</sub> and S-0.2-quasi film **c** Tip<sub>down</sub>, **d** Tip<sub>up</sub>.

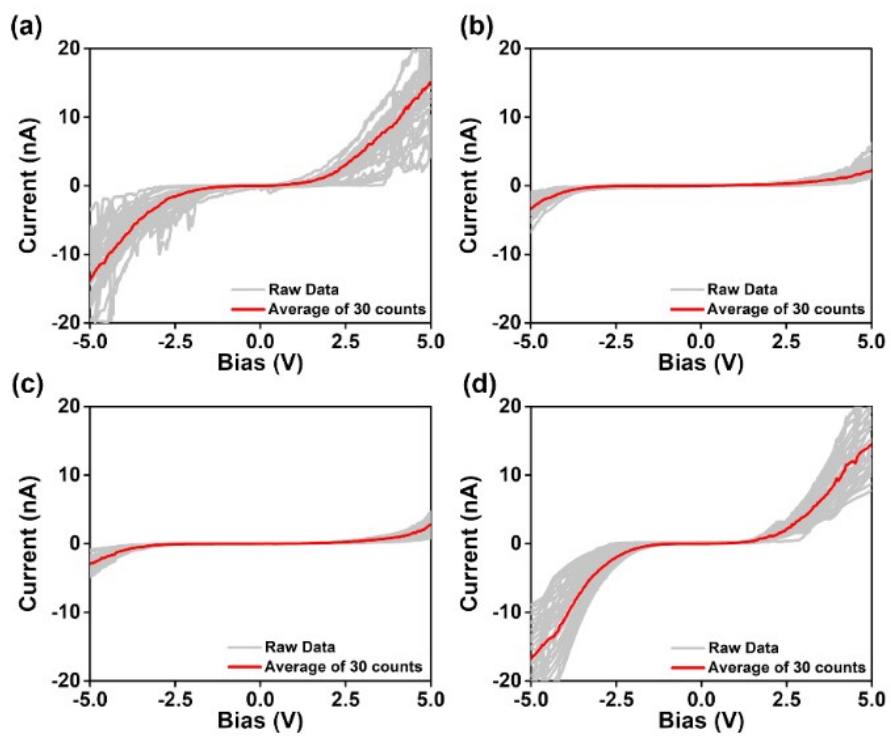


**Fig. S7** Raw and averaged  $I$ - $V$  curves obtained using the mCP-AFM for R-2D film **a** Tip<sub>down</sub>, **b** Tip<sub>up</sub> and S-2D film **c** Tip<sub>down</sub>, **d** Tip<sub>up</sub>.



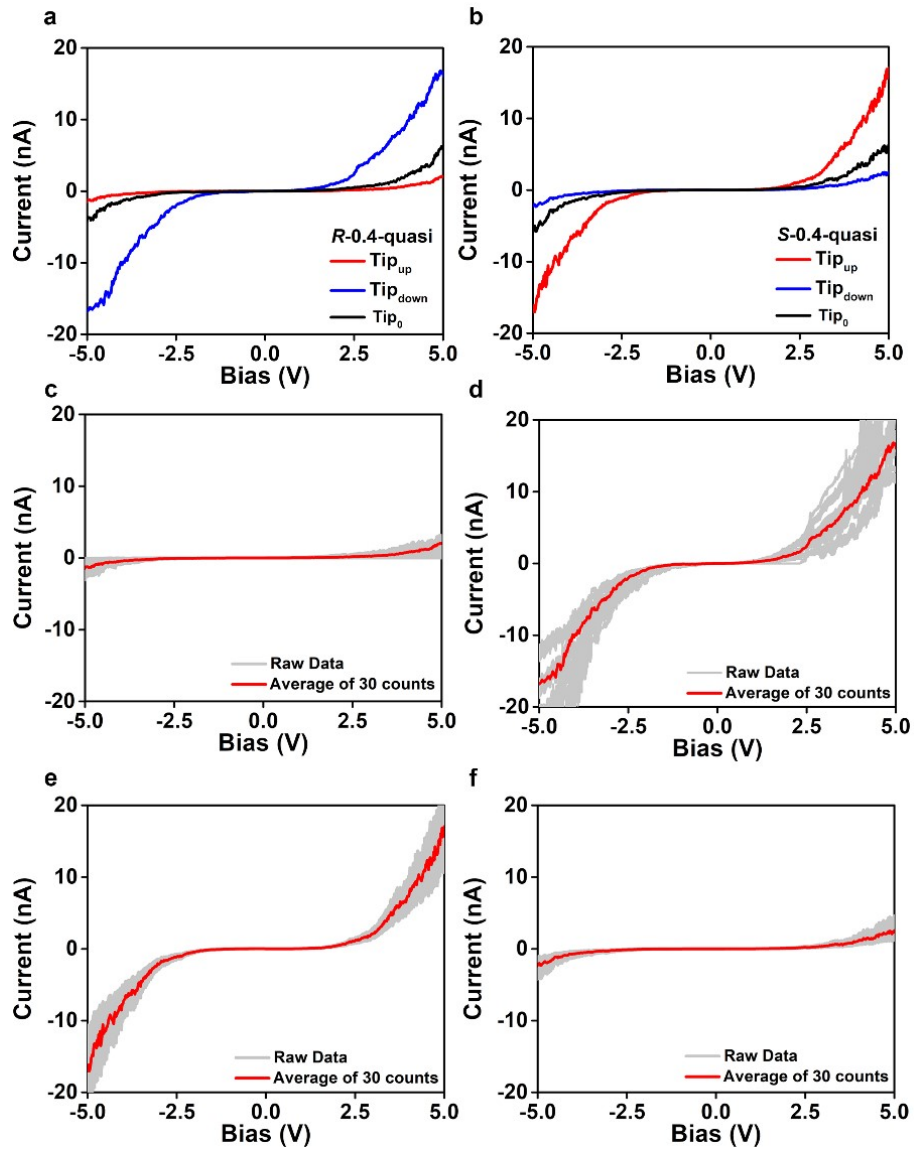


**Fig. S8** Raw and averaged  $I$ - $V$  curves obtained using the mCP-AFM for R-0.4-quasi film **c** Tip<sub>down</sub>, **d** Tip<sub>up</sub> and S-0.4-quasi film **e** Tip<sub>down</sub>, **f** Tip<sub>up</sub>.

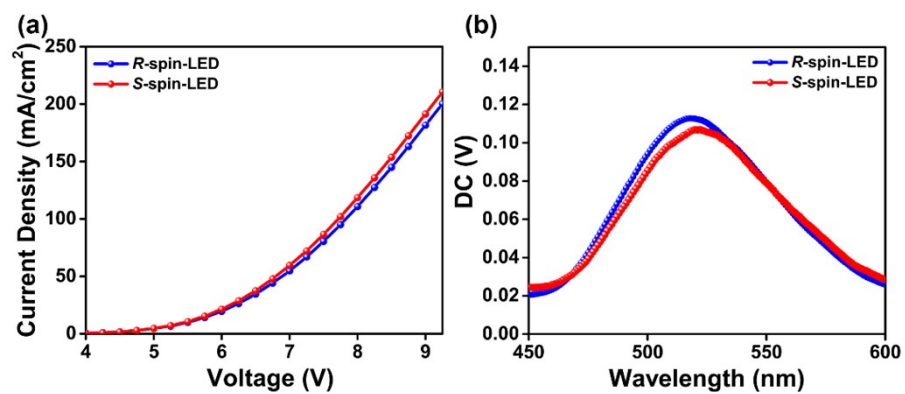


**Fig. S9** Electroluminescence performance of spin-LEDs: **a** Current density-voltage curves of Spin-LEDs. **b** DC spectrum measured at the same time with CP-EL spectrum.

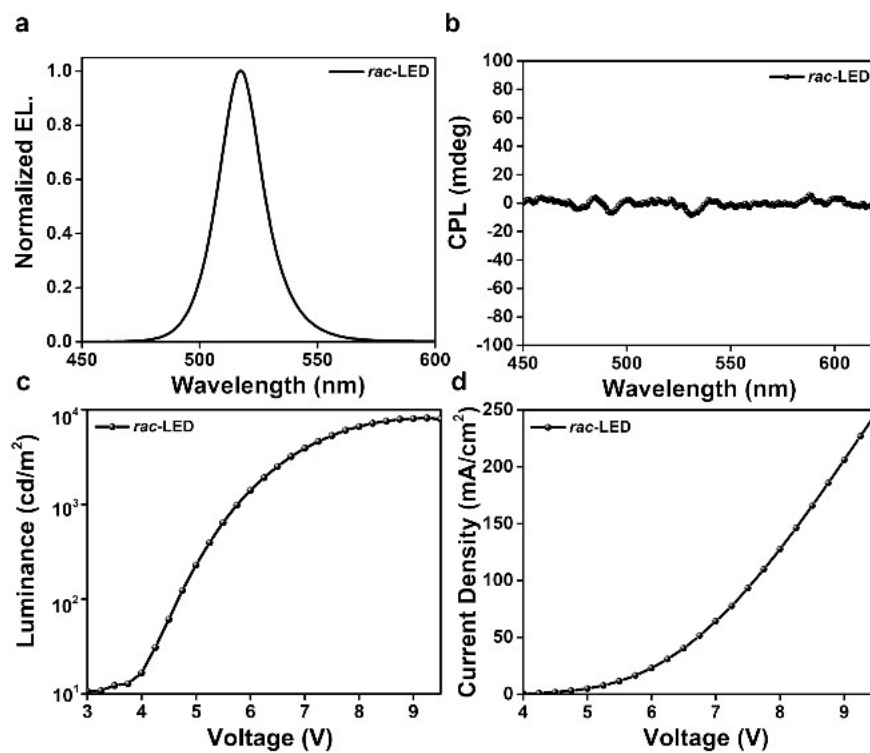


**Fig. S10** Electroluminescence properties of the *rac*-LED: **a** EL spectrum of the *rac*-LED. **b** CP-EL spectrum of the *rac*-LED. **c** Luminance versus voltage curves of the *rac*-LED. **d** Current Density-Voltage curves of *rac*-LED.

**Table S1** Elemental analysis of quasi-2D film

<b>Atomic ratio (%)</b>	<b>C1s</b>	<b>N1s</b>	<b>Br3d</b>	<b>Cs3d5</b>	<b>Pb4f7</b>	<b>N/Pb</b>	<b>Cs/Pb</b>
<i>R</i> -0.4-quasi film	59.47	7.54	23.88	1.28	7.82	0.96	0.16
Precursor	N/A	N/A	N/A	N/A	N/A	1.27	0.33

**Table S2** Summary of CP-EL Emitting LEDs Based on CISS

Spin-LEDs	$ g_{\text{CP-EL}} $	Luminance (cd/m <sup>2</sup> )	EQE (%)	ref
Chiral 2D - achiral 3D	$5.0 \times 10^{-3}$	4200	10.05	1
Chiral core - achiral shell	$6.0 \times 10^{-3}$	1500	3.60	2
Chiral 2D perovskite- achiral CdSe	$1.6 \times 10^{-2}$	18000	2.70	3
Core–Shell Perovskite QD	0.24	1962	5.47	4
This work	0.05	9300	3.80	-

1. Y.-H. Kim, Y. Zhai, H. Lu, X. Pan, C. Xiao, E. A. Gaubling, S. P. Harvey, J. J. Berry, Z. V. Vardeny, J. M. Luther and M. C. Beard, *Science*, 2021, **371**, 1129–1133.
2. C. Ye, J. Jiang, S. Zou, W. Mi and Y. Xiao, *J. Am. Chem. Soc.*, 2022, **144**, 9707-9714.
3. G. Jang, D. Y. Jo, S. Ma, J. Lee, J. Son, C. U. Lee, W. Jeong, S. Yang, J. H. Park, H. Yang and J. Moon, *Adv. Mater.*, 2024, **36**, 2309335.
4. Q. Wang, H. Zhu, Y. Tan, J. Hao, T. Ye, H. Tang, Z. Wang, J. Ma, J. Sun, T. Zhang, F. Zheng, W. Zhang, A. H. W. Choi, W. C. H. Choy, D. Wu, X. W. Sun and K. Wang, *Adv. Mater.*, 2023, **36**, 2305604.